1521-0103/351/2/390–402$25.00
THE JOURNAL OF PHARMACOLOGY AND EXPERIMENTAL THERAPEUTICS

http://dx.doi.org/10.1124/jpet.114.218735
J Pharmacol Exp Ther 351:390–402, November 2014

The Procognitive and Synaptogenic Effects of Angiotensin IV–Derived Peptides Are Dependent on Activation of the Hepatocyte Growth Factor/c-Met System

Caroline C. Benoist, Leen H. Kawas, Mingyan Zhu, Katherine A. Tyson, Lori Stillmaker, Suzanne M. Appleyard, John W. Wright, Gary A. Wayman, and Joseph W. Harding

Department of Integrative Physiology and Neuroscience (C.C.B., L.H.K., M.Z., K.A.T., L.S., S.M.A., J.W.W., G.A.W., J.W.H.) and Department of Psychology (J.W.W., J.W.H.), Washington State University, Pullman, Washington; and M[3] Biotechnology, Inc., Seattle, Washington (L.H.K., J.W.W., J.W.H.)

Received July 29, 2014; accepted September 2, 2014

ABSTRACT

A subset of angiotensin IV (AngIV)–related molecules are known to possess procognitive/antidementia properties and have been considered as templates for potential therapeutics. However, this potential has not been realized because of two factors: 1) a lack of blood-brain barrier–penetrant analogs, and 2) the absence of a validated mechanism of action. The pharmacokinetic barrier has recently been overcome with the synthesis of the orally active, blood-brain barrier–permeable analog *N*-hexanoic-tyrosine-isoleucine-(6) aminohexanoic amide (dihexa). Therefore, the goal of this study was to elucidate the mechanism that underlies dihexa's procognitive activity. Here, we demonstrate that dihexa binds with high affinity to hepatocyte growth factor (HGF) and both dihexa and its parent compound Norleucine 1-AngIV (Nle[1]-AngIV) induce c-Met phosphorylation in the presence of subthreshold concentrations of HGF and augment HGF-dependent cell scattering. Further, dihexa and Nle[1]-AngIV induce hippocampal spinogenesis and synaptogenesis similar to HGF itself. These actions were inhibited by an HGF antagonist and a short hairpin RNA directed at c-Met. Most importantly, the procognitive/antidementia capacity of orally delivered dihexa was blocked by an HGF antagonist delivered intracerebroventricularly as measured using the Morris water maze task of spatial learning.

Introduction

Whereas angiotensin IV (AngIV; VYIHPF) and several AngIV analogs have long been known to possess marked procognitive and antidementia activities (reviewed in Wright and Harding, 2013), questions have persisted regarding their mechanism of action and the identity of the molecular target mediating these effects. In 1992, our laboratory (Harding et al.) reported that a binding site, subsequently referred to as the angiotensin IV receptor subtype (AT_4) bound AngIV with high specificity and affinity. The identity of this protein has been a matter of continuing controversy. One possibility was first offered by Albiston and colleagues (2001) in the form of insulin-regulated membrane aminopeptidase (IRAP). These authors proposed that the physiologic actions of AngIV-related ligands resulted from competitive inhibition of IRAP, thus potentiating the actions of endogenous neuropeptides normally degraded by IRAP. This model predicted that the action of all AngIV-related ligands should be qualitatively equivalent because their action is attributable to competitive interference with IRAP's peptidase activity. This notion is inconsistent with the existence of both agonists and antagonists, which exert opposite physiologic actions (Kramár et al., 1997, 2001; Wright et al., 1999; Hamilton et al., 2001). Further, this model predicts that the physiologic effects of AngIV-related ligands should be slow to materialize because this action requires an accumulation of endogenous ligands. Again this prediction does not agree with the observation that AngIV-related ligands have rapid effects on signaling molecules (Chen et al., 2001; Handa, 2001; Li et al., 2002). Questions surrounding the functional linkage between AngIV-related ligands and IRAP were further amplified by a study that examined the cognitive capabilities of

This work was supported by grants from the Michael J. Fox Foundation and M[3] Biotechnology, Inc. (to J.W.H.); the National Institutes of Health National Institute of Mental Health [Grant R01-MH086032] (to G.A.W.); a Hope for Depression Research Foundation grant (to G.A.W.); a grant from the Edward E. and Lucille I. Lainge Endowment for Alzheimer's Research (to J.W.W.); and the State of Washington.

J.W.H. and J.W.W. are cofounders and major shareholders of M[3] Biotechnology, Inc., which is developing hepatocyte growth factor mimetics and antagonists for the treatment of various disorders including dementia. L.H.K. is the CEO of M[3] Biotechnology, Inc.

C.C.B. and L.H.K. contributed equally to this work.

dx.doi.org/10.1124/jpet.114.218735.

ABBREVIATIONS: aCSF, artificial cerebrospinal fluid; AMPA, α-amino-3-hydroxy-5-methyl-4-isoxazolepropionic acid; AngIV, angiotensin IV (VYIHPF); ANOVA, analysis of variance; AT_4, angiotensin IV receptor subtype; dihexa, *N*-hexanoic-YI-(6) aminohexanoic amide; DIV, day(s) in vitro; HEK-293, human embryonic kidney 293 cell; HGF, hepatocyte growth factor; Hinge, KDYIRN; IRAP, insulin-regulated membrane aminopeptidase; MDCK, Madin-Darby canine kidney cells; mEPSC, miniature excitatory postsynaptic current; mRFP, monomeric red fluorescent protein; norleual, Nle-YL-$\Psi(CH_2\text{-}NH_2)$-HPF; PBS, phosphate-buffered saline; shRNA, short hairpin RNA; α-VGLUT1, vesicular glutamate transporter 1.

IRAP-knockout mice (Albiston et al., 2010). The results of this study indicated that, contrary to the "AngIV/IRAP: inhibition of endogenous peptide metabolism" hypothesis, spatial learning was modestly impaired rather than facilitated as predicted.

If the interaction of AngIV-related peptides with IRAP is not responsible for the profound biologic activities of these molecules, then what is the mechanism? Initial hints of a possible target are apparent in several studies that examined the mechanism of action of "AT_4 receptor antagonists" (Yamamoto et al., 2010; Kawas et al., 2011, 2012), which were originally defined as AngIV-like molecules that interfered with cognition (Wright et al., 1999). These studies demonstrated that the antagonists had structural homology with the dimerization domain of the pleiotropic growth factor hepatocyte growth factor (HGF), bound to HGF with high affinity, blocked HGF's activation and subsequent activation of its receptor c-Met, and displayed both anticancer and antiangiogenic activity as would be expected of an HGF/c-Met antagonist (Peters and Adjei, 2012). While these results clearly linked the action of AT_4-receptor antagonists to the HGF/c-Met system, they did not provide a suitable explanation for the mechanism underlying the procognitive activity of AT_4 receptor agonists.

Thus, the goal of the present study was to provide that explanation. Nle^1-AngIV, an often-employed AT_4 receptor agonist with demonstrated procognitive activity (Benoist et al., 2011), along with its metabolically stabilized and orally active derivative, *N*-hexanoic-tyrosine-isoleucine-(6) aminohexanoic amide (dihexa) (McCoy et al., 2013), were utilized to probe this question. Both agonists were found to potentiate the cellular actions of HGF. Results indicate that it is this ability to activate HGF that is responsible for both the marked synaptogenic and procognitive activities of these compounds.

Materials and Methods

Compounds and Peptide Synthesis

Scopolamine hydrobromide was purchased from Sigma-Aldrich (St. Louis, MO). The peptides were synthesized using Fmoc-based solid-phase peptide synthesis methods and purified by reverse phase high-performance liquid chromatography in the Harding laboratory. Purity and structure were verified by liquid chromatography–mass spectrometry. HGF was purchased from R&D Systems (Minneapolis, MN). [^{3}H]Dihexa with a specific activity of 33.5 Ci/mmol and a high-performance liquid chromatography purity >99% was custom synthesized by ViTrax (Placentia, CA).

Animals and Surgery

Male Sprague-Dawley rats (Taconic-derived) weighing 390–450 g were maintained with free access to water and food (Teklad F6 rodent diet; Harland, Madison, WI), except the night prior to surgery when food was removed. Each animal was anesthetized with ketamine hydrochloride plus xylazine (100 and 2 mg/kg i.m., respectively; Phoenix Scientific, St. Joseph, MO, and Moby, Shawnee, KS). An intracerebroventricular guide cannula (PE-60; Clay Adams, Parsippany, NJ) was stereotaxically positioned (Model 900; David Kopf Instruments, Tujunga, CA) in the right hemisphere using flat skull coordinates 1.0 mm posterior and 1.5 mm lateral to bregma. The guide cannula measured 2.5 cm in overall length and was prepared with a heat bulge placed 2.5 mm from its beveled tip, thus acting as a stop to control the depth of penetration. Once in position, the cannula was secured to the skull with two stainless-steel screws and dental cement. Postoperatively, the animals were housed individually in an American Accreditation for Laboratory Animal Care–approved vivarium maintained at 22 ± 1°C on a 12-hour alternating light/dark cycle initiated at 6:00 AM. All animals were hand-gentled for 5 days.

Behavioral Testing

The water maze consisted of a circular tank painted black (diameter: 1.6 m; height: 0.6 m), filled to a depth of 26 cm with 26–28°C water. A black circular platform (diameter: 12 cm; height: 24 cm) was placed 30 cm from the wall and submerged 2 cm below the water surface.

The maze was operationally sectioned into four equal quadrants designated NW, NE, SW, and SE. For each rat, the location of the platform was randomly assigned to one of the quadrants and remained fixed throughout the duration of training. Entry points were at the quadrant corners (i.e., N, S, E, and W) and were pseudo-randomly assigned such that each trial began at a different entry point than the preceding trial. Three of the four testing room walls were covered with extra-maze spatial cues consisting of different shapes (circles, squares, triangles) and colors. The swimming path of the animals was recorded using a computerized video tracking system (Chromotrack; San Diego Instruments, CA). The computer displayed only total swim latency.

Each member of the treatment groups received an intracerebroventricular injection of scopolamine hydrobromide [70 nmol in 2 μl artificial cerebrospinal fluid (aCSF) over a duration of 20 seconds) or aCSF (control) 20 minutes prior to testing followed by oral dihexa (2 mg/kg per day) or saline (control). When employed, Hinge (KDYIRN; 300 pmol in 2 μl aCSF), or aCSF (control) was delivered by intracerebroventricular injection 5 minutes prior to testing. The behavioral testing protocol has been described previously in detail (Wright et al., 1999). Briefly, acquisition trials were conducted on 8 consecutive days with five trials/day. On the first day of training, the animal was placed on the pedestal for 30 seconds prior to the first trial. Trials commenced with the placement of the rat facing the wall of the maze at one of the assigned entry points. The rat was allowed a maximum of 120 seconds to locate the platform. Once the animal located the platform, it was permitted a 30-second rest period on the platform. If the rat did not find the platform, the experimenter placed the animal on the platform for the 30-second rest period. The next trial commenced immediately following the rest period. Upon completion of each daily set of trials, the animal was towel-dried and placed under a 100-watt lamp for 10–15 minutes and then returned to its home cage.

Dendritic Spine Analysis

Hippocampal Cell Culture Preparation. Hippocampal neurons (2×10^5 cells per square cm) were cultured from P1 Sprague-Dawley rats on plates coated with poly-L-lysine from Sigma-Aldrich (molecular weight: 300,000). Hippocampal neurons were maintained in Neurobasal A media from Invitrogen (Carlsbad, CA) supplemented with B27 from Invitrogen, 0.5 mM L-glutamine, and 5 mM cytosine-D-arabinofuranoside from Sigma-Aldrich added on the second day in culture. Hippocampal neurons were then cultured a further 3–7 days, at which time they were either transfected or treated with various pharmacologic reagents as described in Wayman et al. (2008).

Transfection. Neurons were transfected with monomeric red fluorescent protein (mRFP)–β-actin on day in vitro 6 (DIV6) using Lipofectamine 2000 (Invitrogen) according to the manufacturer's protocol. This protocol yielded the desired 3–5% transfection efficiency, thus enabling the visualization of individual neurons. Higher efficiencies obscured the dendritic arbor of individual neurons. Expression of fluorescently tagged actin allowed clear visualization of dendritic spines, as dendritic spines are enriched in actin. On DIV7, the cells were treated with vehicle (H_2O) or peptides (see Fig. 4) added to the media. On DIV12, the neurons were fixed (4% paraformaldehyde, 3% sucrose, 60 mM PIPES, 25 mM HEPES, 5 mM EGTA, 1 mM $MgCl_2$, pH 7.4) for 20 minutes at room temperature and mounted.

Slides were dried for at least 20 hours at 4°C and fluorescent images were obtained with Slidebook 4.2 Digital Microscopy Software driving an Olympus IX81 inverted confocal microscope with a 60× oil immersion lens, numerical aperture 1.4, and resolution 0.280 μm. Dendritic spine density was measured on primary and secondary dendrites at a distance of at least 150 μm from the soma. Five 50-μm-long segments of dendrites from at least 10 neurons were analyzed for each data point reported.

Each experiment was repeated at least three times using independent culture preparations. Spines were manually counted. Spines were considered dendritic protrusions if they had actin-rich heads with a diameter 1.5 times that of the protrusion shaft.

Organotypic Hippocampal-Slice Culture Preparation and Transfection. Hippocampi from P4 Sprague-Dawley rats were cultured as previously described (Wayman et al., 2006). In order to visualize dendritic arbors 400-μm hippocampal slices from postnatal day 5 were cultured for 3 days, after which they were biolistically transfected with Tomato fluorescent protein using a Helios Gen Gun (Bio-Rad, Hercules, CA) according to the manufacturer's protocol. Following a 24-hour recovery period, slices were stimulated with vehicle (H_2O), 1 pM Nle^1-AngIV, or dihexa for 2 days. Slices were fixed and mounted. Hippocampal CA1 neuronal processes were imaged and measured as described above.

Immunocytochemistry. Transfected neurons were treated and fixed as described above. Following fixation, cells were permeabilized with 0.1% Triton X-100 detergent (Bio-Rad), blocked with 8% bovine serum albumin (InterGen, Burlington, MA) in phosphate-buffered saline (PBS) followed by an incubation period with anti–α-vesicular glutamate transporter (VGLUT)1 (Synaptic Systems, Goettingen, Germany), anti-synapsin (Synaptic Systems), and anti–PSD-95 (Millipore, Billerica, MA) following the manufacturer's protocol, at 4°C. Subsequently cells were rinsed twice with PBS, incubated in Alexa Fluor 488 goat anti-mouse following the manufacturer's protocol (Invitrogen) for 2 hours at room temperature, rinsed again with PBS, and mounted with ProLong Gold Antifade Reagent (Invitrogen). Imaging and analysis were performed as described under "Transfection."

Whole-Cell Recordings. Patch-clamp experiments were performed on mRFP-β-actin–transfected cultured hippocampal neurons with PBS (vehicle control) or 1 pM Nle^1-AngIV pretreatment. Recordings were made on DIV12–14. The culture medium was exchanged by an extracellular solution containing (in mM) 140 NaCl, 2.5 KCl, 1 $MgCl_2$, 3 $CaCl_2$, 25 glucose, and 5 HEPES; pH was adjusted to 7.3 with KOH; and osmolality was adjusted to 306–310 mOsm. Cultures were allowed to equilibrate in a recording chamber mounted on an inverted microscope (IX71; Olympus Corporation, Tokyo, Japan) for 30 minutes before recording. Transfected cells were visualized with fluorescence (Olympus Corporation). Recording pipettes were pulled (P-97 Flaming/Brown Micropipette Puller; Sutter Instrument, Novato, CA) from standard wall borosilicate glass without filament (optical density: 1.5 mm; Sutter Instrument). The resistance of patch electrodes ranged from 4.0 to 5.2 MΩ, and were filled with an internal solution of the following composition (in mM): 25 CsCl, 100 $CsCH_3O_3S$, 10 phosphocreatine, 0.4 EGTA, 10 HEPES, 2 $MgCl_2$, 0.4 Mg-ATP, and 0.04 Na-GTP; pH was adjusted to 7.2 with CsOH; osmolality was adjusted to 298–300 mOsm. Miniature excitatory postsynaptic currents (mEPSCs) were isolated pharmacologically by blocking $GABA_A$ receptor channels with picrotoxin (100 μM; Sigma-Aldrich), glycine receptors with strychnine (1 μM; Sigma-Aldrich), and sodium channels with tetrodotoxin (500 nM; R&D Systems). Recordings were obtained using a Multiclamp 700B amplifier (Molecular Devices, Sunnyvale, CA). Analog signals were low-pass Bessel filtered at 2 kHz, digitized at 10 kHz through a Digidata 1440A interface (Molecular Devices), and stored in a computer using Clampex 10.2 software (Molecular Devices). The membrane potential was held at –70 mV at room temperature (25°C) during a period of 0.5–2 hours after removal of the culture from the incubator. Liquid junction potentials were not corrected. Data analysis was performed using Clampfit 10.2 software, and Mini Analysis 6.0 software (Synaptosoft Inc., Fort Lee, NJ). The criteria for a successful recording included an electrical resistance of the seal between the outside surface of the recording pipette and the attached cell >2 GΩ and a neuron input resistance >240 MΩ. The mEPSCs had a 5-minute recording time.

HGF Binding

The binding of [^{3}H]dihexa to HGF was assessed using a soluble-binding assay. Saturation isotherms were developed for the interaction of [^{3}H]dihexa with HGF. Human HGF (1.25 ng) in 250 μl PBS were incubated with multiple concentrations of [^{3}H]dihexa ranging from 10^{-13} M to 10^{-8} for 40 minutes at 37°C. Preliminary kinetic studies indicated that equilibrium binding was reached by 40 minutes of incubation at 37°C. The incubates were then spun through Bio-Gel P6 (Bio-Rad) spin columns (400-μl packed volume) for 1 minute to separate free and bound [^{3}H]dihexa and the eluent collected. Five milliliters of scintillation fluid was added to the eluent that contained the HGF-bound [^{3}H]dihexa, and then counted using a scintillation counter. Total disintegrations per minute of bound [^{3}H]dihexa were calculated based on machine counting efficiency. Saturation isotherms were performed in quadruplicate. The affinity of [^{3}H]dihexa for HGF (K_d) and total binding (B_{max}) were determined, using the Prism 5 and InStat v.3.05 graphical/statistical programs (GraphPad, San Diego).

Dimerization

HGF dimerization was assessed using PAGE followed by silver staining. Human HGF, at a concentration of 0.08 ng/μl with or without drugs, was incubated with heparin at a final concentration of 5 μg/ml. Twenty-five millimolar bissulfosuccinimidyl suberate cross-linker (Thermo Fisher Scientific/Pierce Protein Biology Products, Rockford, IL) was then added to the reaction for 30 minutes at 37°C. Subsequently, the reaction was quenched with 20 mM Tris buffer. Qualitatively identical results were also obtained in the absence of bissulfosuccinimidyl suberate, attesting to the high affinity of the HGF/HGF dimer. Loading buffer was then added to each sample and the mixture separated by native PAGE using gradient Criterion XT precast gels (4–12% Bis-Tris; Bio-Rad). Similar results were obtained in the presence of SDS. Next, the gel was silver-stained for the detection of the HGF monomers and dimers. Bands were quantitated from digital images using a UVP Inc. PhosphorImager (Upland, CA).

Western Blotting

Human embryonic kidney (HEK)-293 cells were seeded in six-well tissue culture plates and grown to 95% confluency in Dulbecco's modified Eagle's medium containing 10% fetal bovine serum. The cells were serum-deprived for 24 hours prior to the treatment to reduce the basal levels of phospho-Met. Following serum starvation, cocktails composed of vehicle and HGF with/without dihexa or Nle^1-AngIV were prepared and preincubated for 30 minutes at room temperature. The cocktail was then added to the cells for 10 minutes to stimulate the Met receptor activation. Cells were harvested using radioimmunoprecipitation assay lysis buffer supplemented with phosphatase inhibitor cocktails 1 and 2 (Sigma-Aldrich). The lysate was clarified by centrifugation at 15,000*g* for 15 minutes, protein concentrations were determined using the BCA Total Protein Assay (Pierce), and then appropriate volumes of the lysates were diluted with 2× reducing Laemmli buffer and heated for 10 minutes at 95°C. Samples containing identical amounts of protein were resolved using SDS-PAGE (Criterion; Bio-Rad), transferred to nitrocellulose, and blocked in Tris-buffered saline containing 5% milk for 1 hour at room temperature. The phospho-Met antibody or total Met antibody was added to the blocking buffer at a final concentration of 1:1000 and incubated at 4°C overnight with gentle agitation. The membranes were then washed several times with water and Tris-buffered saline with 0.05% Tween-20, a 1:5000 dilution of horseradish peroxidase–conjugated goat anti-rabbit antiserum was added, and the membranes further incubated for 1 hour at room temperature. Proteins were visualized using the Supersignal West Pico Chemiluminescent Substrate system (Thermo/Pierce) and molecular weights determined by comparison to protein ladders (BenchMark; Invitrogen; and Kaleidoscope; Bio-Rad). Images were digitized and analyzed using a UVP PhosphorImager.

Short Hairpin RNA

A target sequence for c-Met was designed using RNAi central design program (http://cancan.cshl.edu/). The target sequence GTGTCAGGAGGTGTTTGGAAAG was inserted into pSUPER vector (Oligoengine,

Seattle, WA), which drives endogenous production of short hairpin RNA (shRNA) under the H1 promoter. The shRNA was transfected into cells using the Lipofectamine method described above. Verification of receptor knockdown was done by creating a c-Met-6-Myc–tagged gene product using the Gateway cloning system (Invitrogen). The Met protein coding sequence was cloned from rat whole brain cDNA using primers obtained from Integrated DNA Technologies (Coralville, IA). The amplified product was gel-purified and a band corresponding to 190 kDa excised and cloned into a pCAGGS-6-Myc destination vector (Gateway).

Scattering Assay

Madin-Darby canine kidney (MDCK) cells were grown to 100% confluency on coverslips in six-well plates and washed twice with PBS. The confluent coverslips were then aseptically transferred to new six-well plates containing 900 μl serum-free Dulbecco's modified Eagle's medium. Nle^1-AngIV, dihexa, and/or HGF (20 ng/ml) were added to appropriate wells. Control wells received PBS vehicle. Plates were incubated at 37°C with 5% CO_2 for 48 hours. Media was removed and cells were fixed with methanol. Cells were stained with Diff-Quik Wright-Giemsa (Dade Behring, Newark, DE) and digital images were taken. Coverslips were removed with forceps and more digital images were captured. Pixel quantification of images was achieved using ImageJ (NIH, Bethesda, MD) and statistics were performed using Prism 5 and InStat v.3.05.

Statistical Analyses

The Morris water maze data sets, consisting of mean latencies and path distances to find the platform during each daily block of five trials, were calculated for each animal for each day of acquisition. Overall differences in learning curves were assessed with two-way analyses of variance (ANOVAs) with repeated measures with Bonferroni correction. Additionally, one-way ANOVAs were used to compare group latencies swum on various days of training. Significant effects were further analyzed by a Newman-Keuls post-hoc test with a level of significance set at $P < 0.05$.

One-way ANOVA was also used to analyze the dendritic spine and electrophysiology results, and significant effects were analyzed by Tukey post-hoc test, with a level of significance set at $P < 0.05$. Numerical data are expressed as mean ± S.E.M.

Results

The AngIV Analog Binds to HGF with High Affinity and Inhibits HGF Dimerization. Previous studies from our laboratory have demonstrated that various AngIV analogs, which act as "AT_4 receptor antagonists" possess structural homology with the dimerization domain of HGF. These analogs bind HGF with high affinity while blocking HGF dimerization and ultimately its capacity to activate c-Met (Kawas et al., 2011, 2012). Furthermore, there appears to be direct correlation between biological activity and the ability to inhibit HGF dimerization (Kawas et al., 2012). While it was easy to envision how an antagonist could exert its effects by blocking the dimerization of HGF, a process linked to its activation (Gherardi et al., 2006; Youles et al., 2008), the same could not be said for structurally similar agonists, especially if they also engaged an HGF-dependent mechanism.

To begin to address this quandary [tyrosine-2,6-^{3}H]dihexa was synthesized and its direct binding to HGF assessed. [^{3}H]Dihexa was found to bind HGF saturably and with high affinity (K_d = 65 pM) (Fig. 1A). The ability of dihexa to bind HGF raised the question of its impact on the dimerization process. To address this question, native gels in combination with silver staining and densitometry were employed to visualize HGF monomers and multimers and quantitate the effect of dihexa, and several representative antagonists in the dimerization process (Fig. 1, B and C). Somewhat surprisingly, dihexa effectively inhibited HGF dimerization at 10^{-10} M concentration, similar to that seem with HGF antagonists, Nle-YL-Ψ(CH_2-NH_2)-HPF (norleual), Hinge, and Norleucine-X-6-aminohexanoic amide family analogs. Although not directly addressed in these studies, these data suggest that dihexa and its parent compound, Nle^1-AngIV, might act allosterically to stabilize an active HGF conformation. Consistent with this hypothesis, we have recently demonstrated that c-Met is premultimerized on the dendrites of hippocampal neurons as dimers, tetramers, hexamers, and octomers in the absence of HGF, suggesting that the HGF dimerization process likely subserves a function other than initiating receptor dimerization (Kawas et al., 2013).

Dihexa and Nle^1-AngIV Act Synergistically with HGF to Augment c-Met Signaling and HGF-Dependent Cellular Activity. The notion that dihexa and Nle^1-AngIV allosterically activate HGF predicts that these analogs should potentiate HGF's ability to activate its receptor and subsequent cellular responses. To evaluate this idea, HEK-293 cells, which express c-Met, were stimulated with threshold levels of HGF in the presence of dihexa and Nle^1-AngIV, and the impact on c-Met activation (phosphorylation) was accessed (Fig. 2). While dihexa at 10^{-10} M and 10^{-12} M alone did not activate c-Met, dihexa at both concentrations markedly augmented the capacity of HGF at 1.25 and 2.5 ng/ml to activate c-Met (Fig. 2, A and B). Similarly these concentrations of Nle^1-AngIV potentiated the ability of 1.25 and 2.5 ng/ml of HGF to activate c-Met (Fig. 2, C and D). However, unlike dihexa, Nle^1-AngIV alone at concentrations of 10^{-10} M and 10^{-12} M was capable of activating c-Met, perhaps suggesting an even higher affinity for HGF than dihexa.

c-Met activation initiates multiple cellular responses, including increased proliferation/survival, motility, and differentiation (Zhang and Vande Woude, 2003). Together, these cellular responses contribute to c-Met's hallmark effect of scattering, a process characterized by decreased cell adhesion and increased motility and proliferation. In order to explore the physiologic significance of dihexa's and Nle^1-AngIV's ability to augment c-Met signaling, we evaluated the effect of dihexa and Nle^1-AngIV on classic c-Met–dependent changes in cell behavior using MDCK cells, a standard cellular model for investigating the HGF/c-Met system (Stella and Comoglio, 1999). Stimulation with dihexa at 10^{-10} M facilitated HGF-dependent scattering, while concentrations of 10^{-12} M and 10^{-14} M produced a dose-dependent trend toward potentiation that did not reach statistical significance (Fig. 3, A and B). Further, in the absence of exogenously applied HGF, dihexa at 10^{-12} M markedly augmented scattering, suggesting the presence of endogenous HGF in the preparation. Consistent with the presence of endogenous HGF in the cultures, Nle^1-AngIV at 10^{-8} M, 10^{-10} M, and 10^{-12} M supported cell scattering in the absence of added exogenous HGF (Fig. 3, C and D). Taken together these data indicate that both dihexa and Nle^1-AngIV at subnanomolar concentrations are capable of potentiating the impact of HGF on both c-Met activation and subsequent cellular responses.

HGF Augments the Dendritic Architecture and Supports Increased Spinogenesis. The ability of dihexa and Nle^1-AngIV to stimulate hippocampal spinogenesis and synaptogenesis (McCoy et al., 2013) and their capacity to facilitate the actions of HGF predicts that HGF itself should enhance spinogenesis and synaptogenesis. As such, the effects of HGF on spinogenesis in dissociated hippocampal cultures were evaluated. To this end, hippocampal neurons were

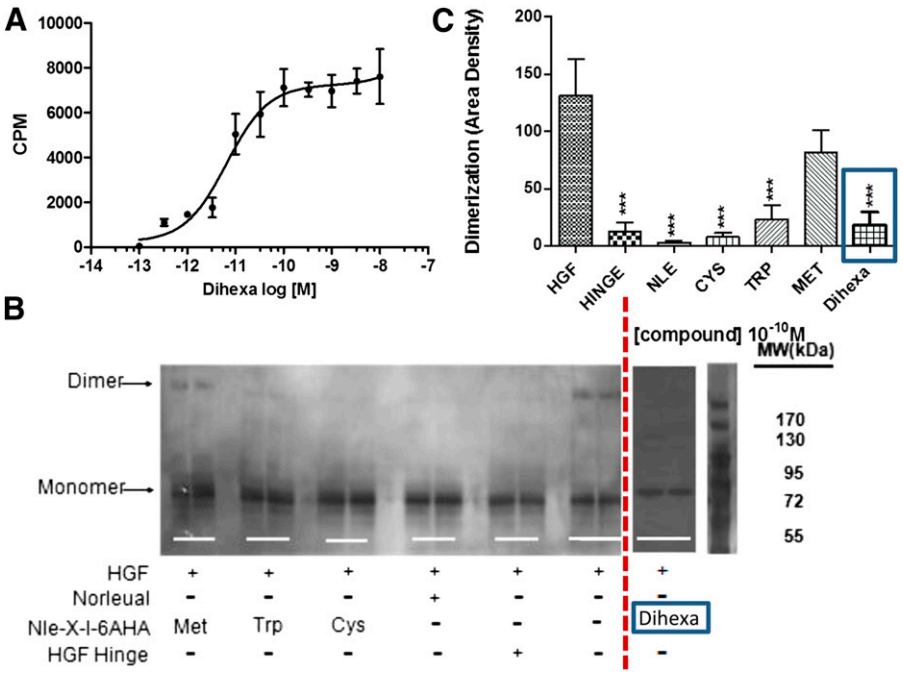

Fig. 1. Binding of the HGF mimetic dihexa to HGF and its impact on HGF dimerization. (A) Dihexa binds saturably and with high affinity to HGF. The binding of [^{3}H]dihexa to HGF was assessed using a soluble binding assay. Saturation isotherms were developed for the interaction of [^{3}H]dihexa with HGF. Human HGF (1.25 ng) in 250 μl of PBS were incubated with multiple concentrations of [^{3}H]dihexa ranging from 10^{-13} M to 10^{-8} for 40 minutes at 37°C. The incubates were then spun through Bio-Gel P6 spin columns (400 μl packed volume) for 1 minute to separate free and bound [^{3}H]dihexa and the eluent collected and counted. Graph is a composite of three experiments run in quadruplicate. $N = 3$, mean ± S.E.M. ($K_d = 6.52 \times 10^{-11}$ M). (B) Dihexa blocks HGF dimerization. HGF dimerization was assessed in the presence of various analogs including dihexa. Norleual, the Nle-X-6AHA (Cys, Met, Trp) analogs, and HGF Hinge have been shown to be HGF antagonists (Yamamoto et al., 2010; Kawas et al., 2011, 2012). Dimerization was carried out for 30 minutes in the presence of heparin. Samples where crosslinked with bissulfosuccinimidyl suberate (BS3) and separated by native PAGE. Bands were visualized by silver staining and (C) quantitated by densitometry. ($N = 6$; $^{***}P < .001$.) [Some of the data in (B) was previously published (Kawas et al., 2012) and is being presented for comparison purposes.] CPM, counts per minute.

transfected with mRFP-β-actin on DIV6, stimulated with HGF for 5 days, and subsequently analyzed for the number of dendritic spines.

A dose-dependent increase in spine numbers following HGF stimulation was observed, with a lowest effective dose of 5 ng/ml (mean spine numbers = 24.7; $^{**}P < 0.01$ versus control; not significant at $P > 0.05$, versus HGF 10 and 20 ng/ml). The most significant effects were produced by 10- and 20-ng/ml doses (mean spine numbers = 27.5 and 27.0 respectively; $n = 50$ per treatment group; $^{***}P < 0.001$; df = 4/245; F = 13.5). However, the 2.5-ng/ml dose of HGF had no effect on basal spine numbers (mean spine numbers = 18.6 versus control = 18.0) (Fig. 4A) and was therefore considered to be subthreshold.

To further confirm the ability of HGF to augment spinogenesis in a more anatomically intact environment, HGF-dependent spinogenesis in organotypic hippocampal slices was examined and compared with dihexa. Hippocampal slices were biolistically transfected with the soluble red fluorescent protein Tomato and stimulated with 10 ng/ml HGF, 10^{-12} M dihexa, or vehicle for 48 hours. CA1 hippocampal neurons, which are known to undergo plastic changes in response to learning and can be easily identified by their location and morphological characteristics, were evaluated for changes in spine numbers. Both dihexa and HGF significantly increased the number of spines per 50-μm dendrite length in the CA1 hippocampal neurons (mean spine numbers = 15.0 and 18.5, respectively, compared to mean control spine numbers = 6.1; $^{***}P < 0.001$ and $^{**}P < 0.01$ between treatment groups; df = 2/81; F = 41.5) (Fig. 4, B and C).

Dihexa and Nle^1-AngIV Act Synergistically with HGF to Increase Hippocampal Neuron Spinogenesis. The capacity of dihexa and Nle^1-AngIV to shift the HGF dose-response curve to the left in HEK-293 cells coupled with their ability to augment spinogenesis in hippocampal neurons further anticipated that dihexa and Nle^1-AngIV should similarly potentiate the spinogenic activity of HGF. To test this notion the combined effects of subthreshold doses of HGF augmented with dihexa or Nle^1-AngIV were evaluated in dissociated rat hippocampal neurons. Dissociated hippocampal neurons transfected with mRFP-β-actin were stimulated for 5 days with subthreshold concentrations of HGF and dihexa or Nle^1-AngIV (2.5 ng/ml + 10^{-13} M, respectively). Additionally, biologically active doses of HGF (10 ng/ml), dihexa, or Nle^1-AngIV (10^{-12} M), or a combination of subthreshold doses of 2.5 ng/ml HGF + 10^{-13} M dihexa or 2.5 ng/ml HGF + 10^{-13} M Nle^1-AngIV were applied.

As expected, putative subthreshold concentrations of HGF (2.5 ng/ml), dihexa, and Nle^1-AngIV (10^{-13} M) failed to alter basal spinogenesis and did not differ from control-treated neurons (mean ± S.E.M. spine numbers for control = 17.4, HGF = 16.5, dihexa = 17.1 and Nle^1-AngIV = 16.5 per 50-μm dendrite length; $P > 0.05$). In contrast, biologically active doses of HGF (10 ng/ml), dihexa, and Nle^1-AngIV (10^{-12} M) produced a significant effect over control treated spines (mean ± S.E.M. spine numbers for HGF = 29.3, dihexa = 26.4 and Nle^1-AngIV = 29.8 per 50-μm dendrite). Combined subthreshold doses of 2.5 ng/ml HGF + 10^{-13} M dihexa and 2.5 ng/ml HGF + 10^{-13} M Nle^1-AngIV phenocopied the effects of each agonist at its biologically active dose alone (mean ± S.E.M. spine numbers

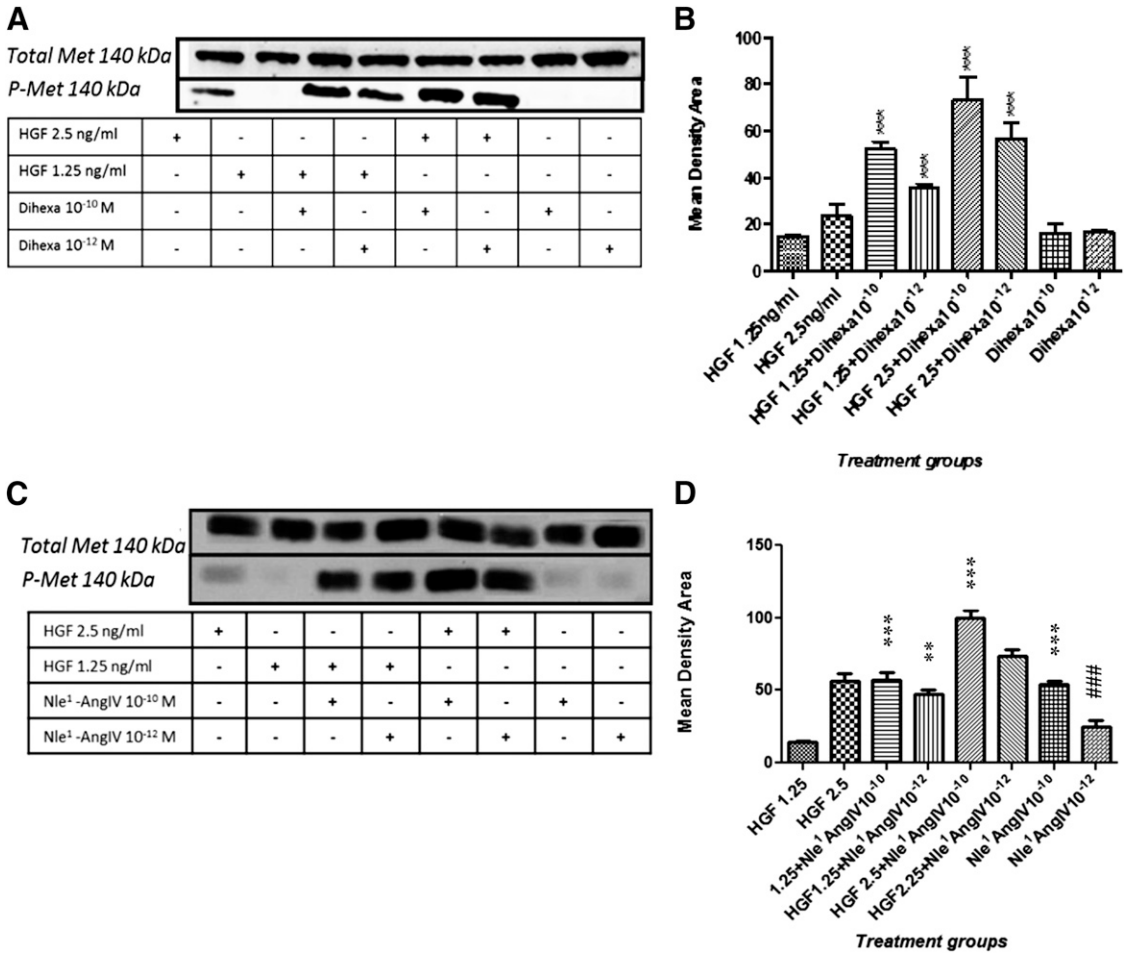

Fig. 2. The HGF mimetics dihexa and Nle[1]-AngIV allosterically regulate HGF, resulting in c-Met activation. The effect of dihexa and Nle[1]-AngIV on HGF-dependent c-Met activation was assessed in HEK-293T cells and analyzed for phosphorylated (activated) and total c-Met by immunoblotting. (A) An SDS-PAGE illustrates the impact of dihexa at 10^{-10} M and 10^{-12} M on HGF-dependent c-Met phosphorylation. (B) Dihexa at 10^{-10} M augmented the effect of HGF at 1.25 ng/ml ($P < 0.001$) and 2.5 ng/ml ($P < 0.001$). Similarly, dihexa at 10^{-12} M augmented HGF's activity at 1.25 ng/ml ($P < 0.001$) and 2.5 ng/ml ($P < 0.001$). Neither dihexa at 10^{-10} M nor at 10^{-12} M stimulated c-Met phosphorylation beyond background. No significant change in total c-Met was observed in any experimental group. $N = 4$; mean ± S.E.M. (C) An SDS-PAGE illustrates the impact of Nle[1]-AngIV at 10^{-10} M and 10^{-12} M on HGF-dependent c-Met phosphorylation. (D) Nle[1]-AngIV at 10^{-10} M (***$P < 0.001$) and 10^{-12} M (**$P < 0.01$) augmented the effect of HGF at 1.25 ng/ml, and Nle[1]-AngIV at 10^{-10} M and 10^{-12} M augmented HGF's activity at 2.5 ng/ml (***$P < 0.001$). Nle[1]-AngIV alone at 10^{-10} M stimulated c-Met phosphorylation beyond background ($P < 0.05$) while Nle[1]-AngIV at 10^{-12} M was not different from background (###$P > 0.05$). No significant change in total c-Met was observed in any experimental group. $N = 4$; mean ± SEM. Together these data demonstrate the capacity of HGF mimetics to shift the dose-response curve of HGF's activation of c-Met to the left.

for HGF + dihexa are 28.8 and HGF + Nle[1]-AngIV are 26.2 per 50-μm dendrite length compared to control treated neurons = 17.4; ***$P < 0.001$; mean ± S.E.M.; by one-way ANOVA followed by Tukey post hoc test). Together these data (Fig. 4, D and E) further confirm that HGF and the HGF activators dihexa and Nle[1]-AngIV act synergistically, resulting in significant changes in neuronal structure.

Dihexa, Nle[1]-AngIV, and HGF Support the Development of Functional Synapses. Previous studies in which neurons were treated with dihexa and Nle[1]-AngIV indicated that most of the induced dendritic spines were colocalized with both pre- and postsynaptic markers indicative of functional synapses (Benoist et al., 2011; McCoy et al., 2013). Additionally the majority of synaptic input appeared to be glutamatergic. Because it has been suggested that dihexa and Nle[1]-AngIV operate via an HGF-dependent mechanism, the functional properties of HGF-induced spines were evaluated. mRFP-β-actin–transfected hippocampal neurons were immunostained for a general marker of presynaptic active zones, synapsin (Ferreira and Rapoport; 2002), as well as a marker specific for glutamatergic synapses, VGLUT1 (Balschun et al., 2010). HGF stimulation significantly augmented the number of postsynaptic spines (Fig. 4A). The number of postsynaptic spines (red) adjacent to VGLUT1, or synapsin-positive puncta (green) were counted and converted to a percentage of the total spines counted. For HGF-treated neurons (10 ng/ml) immunostained with anti-synapsin1, 98% of the actin-enriched spines codistributed with synapsin1 (Fig. 5, A and B). Similarly, 95% of the spines codistributed with VGLUT1, indicating that spines induced by HGF were almost exclusively glutamatergic (Fig. 5, A and C). The codistribution of green puncta representative of synapsin1 and VGTUT1 and mRFP-β-actin–labeled spines for vehicle-treated neurons exhibited a parallel 94% correlation (Fig. 5, A and D). The above data suggest that spines produced in response to HGF treatment form functional synapses. Furthermore, the high correlation with VGLUT1 suggests that many of these inputs are excitatory in nature.

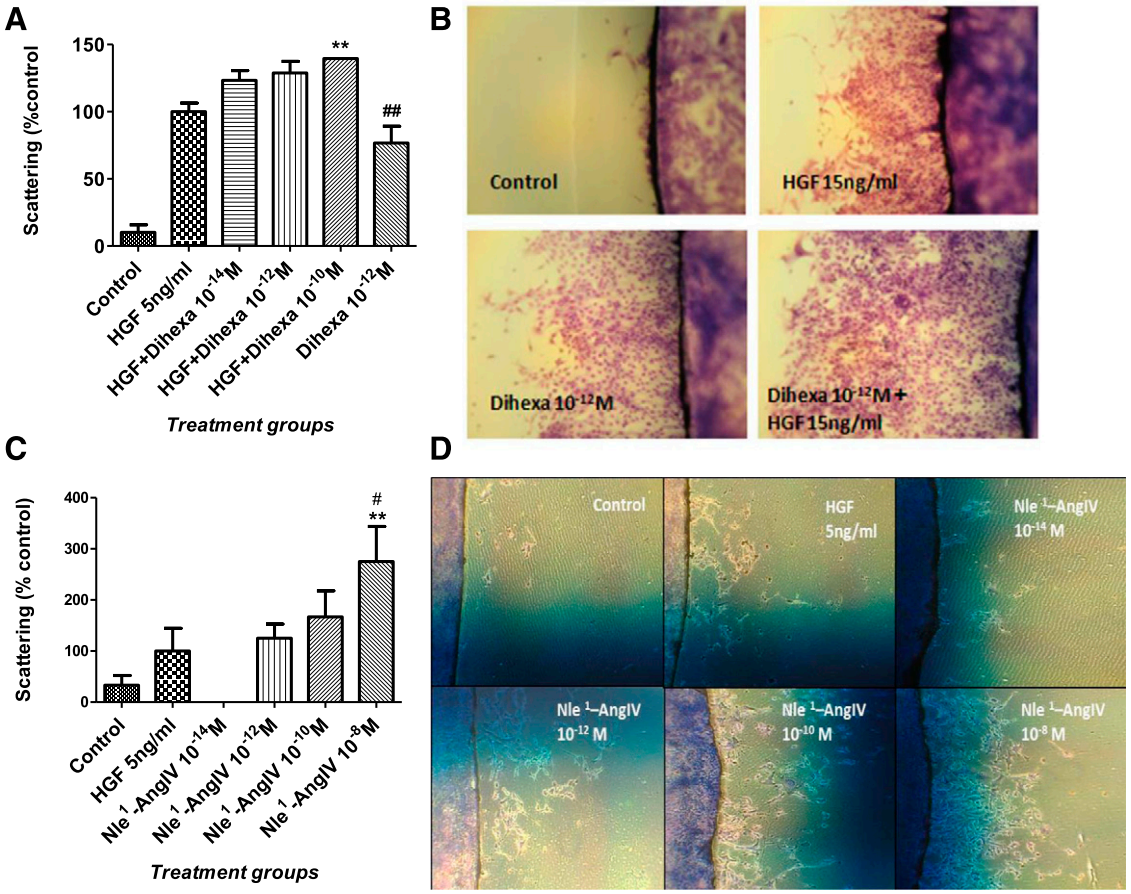

Fig. 3. Effect of the HGF mimetics dihexa and Nle[1]-AngIV on HGF-dependent cell scattering. Cell scattering was assessed in MDCK cells. Cells were grown to confluence on coverslips, which were then transferred to a clean plate. HGF, dihexa, or Nle[1]-AngIV alone or in combination was then added to the media at various concentrations. After treatment for 4 days, the number of cells that had scattered off the coverslip was quantitated. (A) HGF at 5 ng/ml significantly stimulated cell scattering ($P < 0.001$). The addition of dihexa at 10^{-10} M further increased scattering (**$P < 0.01$). Dihexa alone at 10^{-12} M was able to enhance scattering ($P < 0.01$). Examples of the effect of dihexa are illustrated in (B). Nle[1]-AngIV at 10^{-8} M, 10^{-10} M, and 10^{-12} M stimulated cell scattering (# and **$P < 0.05$–0.01). Nle[1]-AngIV at 10^{-14} M had no effect on scattering (C). Examples of the effect of dihexa are illustrated in (D).

To further validate the conclusion that new spines supported functional synapses, we measured the frequency of spontaneous AMPA (α-amino-3-hydroxy-5-methyl-4-isoxazolepropionic acid) receptor–mediated mEPSCs from neurons following HGF treatment and compared the data to that obtained for dihexa, which had been previously established to increase the number of morphologically identified synapses with a concomitant rise in the frequency of mEPSCs (McCoy et al., 2013). Recordings were made in dissociated hippocampal neurons transfected with mRFP-β-actin and treated with 10^{-12} M dihexa, 10 ng/ml HGF, or an equivalent volume of vehicle following 5 days of drug exposure. Both HGF (mean frequency = 5.84 ± 0.68; $n = 9$) and dihexa treatment (mean frequency = 5.32 ± 1.01; $n = 9$) increased mEPSC frequency approximately 2-fold over control-treated neurons [mean frequency = 2.19 ± 0.75; $n = 9$; ***$P < 0.012$ (HGF), and $P < 0.04$ (dihexa); mean ± S.E.M. by one-way ANOVA followed by Tukey post hoc test] (Fig. 5E), supporting the supposition that HGF treatment increases synaptogenesis.

HGF Antagonist Hinge and a c-Met–Specific shRNA Block the Biologic Actions of HGF, Dihexa, and Nle[1]-AngIV. Seeking further substantiation that the actions of dihexa and Nle[1]-AngIV are mediated through the HGF/c-Met system, the novel HGF antagonist Hinge (KDYIRN) and an shRNA targeting c-Met were employed to block the spinogenic and synaptogenic effects of dihexa and Nle[1]-AngIV. Hinge had previously been validated as an HGF antagonist by its ability to inhibit HGF-dependent c-Met phosphorylation and HGF-dependent cellular responses, including scattering of MDCK cells (Kawas et al., 2011).

Hinge alone was found to have no effect on spinogenesis over a wide range of doses (10^{-8} M to 10^{-12} M) in dissociated hippocampal neurons, thus suggesting that Hinge and the HGF/c-Met system do not have a significant role in the basal spinogenesis seen in the cultured neurons. However, Hinge was effective at inhibiting spine formation in neurons stimulated with 10 ng/ml HGF (Fig. 6A), 10^{-12} M dihexa (Fig. 6B), or 10^{-12} M Nle[1]-AngIV (Fig. 6C), further supporting the contention that these actions are mediated by the HGF/c-Met system.

To assess the effects of Hinge on glutamate inputs, mEPSCs were recorded from mRFP-β-actin–transfected hippocampal neurons treated for 5 days with Hinge (10^{-12} M), HGF (10 ng/ml), dihexa (10^{-12} M), Hinge + HGF (10^{-12} M + 10 ng/ml, respectively), or Hinge + dihexa (10^{-12} M each) (Fig. 6, D and E). Hinge alone did not affect mEPSC frequency [mean frequency = 3.96 ± 0.29, $n = 38$ (Fig. 6D), and 4.00 ± 0.37, $n = 23$ (Fig. 6E)] compared to vehicle-treated neurons [mean frequency = 4.81 ± 0.32, $n = 44$ (Fig. 6D), and 3.72 ± 0.28, $n = 44$ (Fig. 6E)]. HGF and dihexa significantly increased mEPSC frequency compared to both

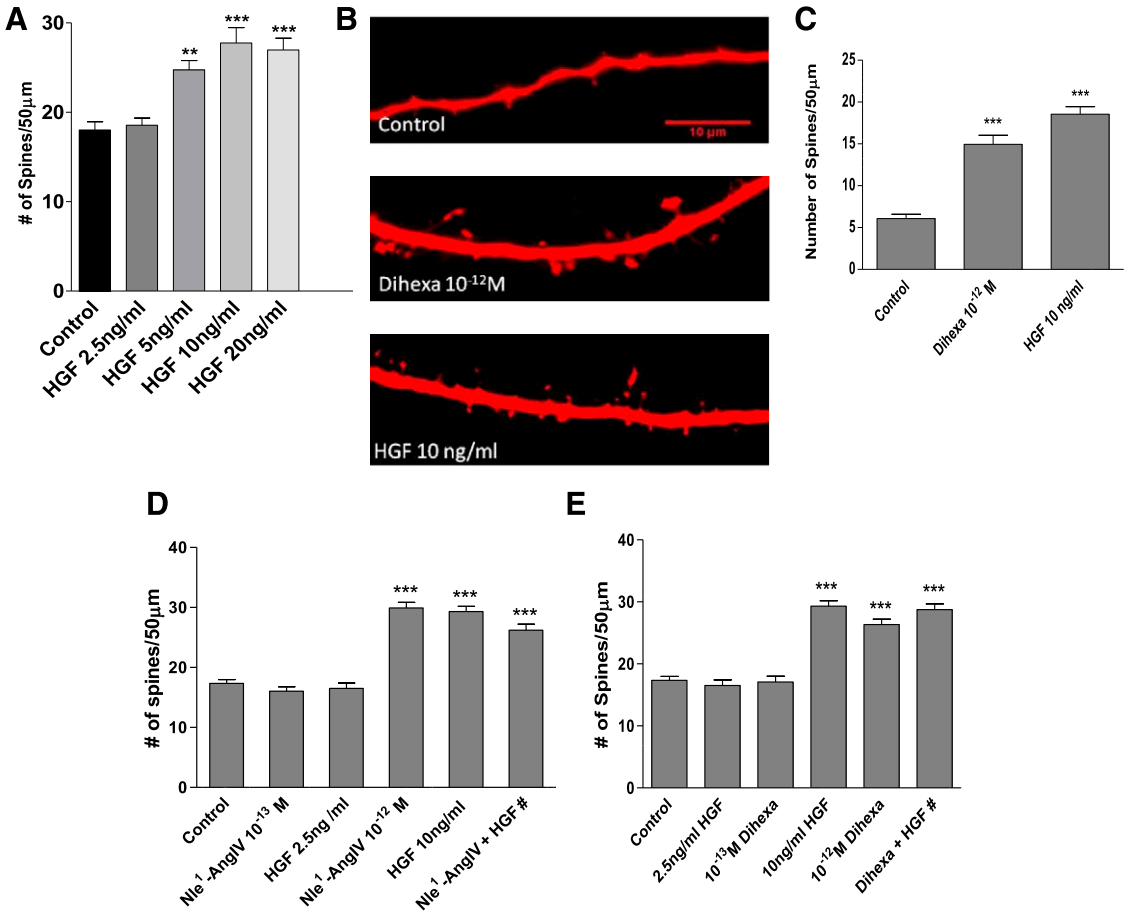

Fig. 4. (A) HGF dose dependently enhances spinogenesis. Dissociated hippocampal neurons from 1- or 2-day-old rats were transfected with mRFP-β-actin and stimulated with HGF for 5 days. Treatment with 2.5 ng/ml of HGF did not affect basal spine numbers and was considered subthreshold. Doses of 5, 10, and 20 ng/ml significantly increased the number of spines per 50-μm dendrite lengths compared to vehicle control–treated neurons. ***$P < 0.001$; **$P < .01$; Mean ± S.E.M.; $N = 50$ per treatment group. (B and C) Effects of dihexa and HGF on spinogenesis in organotypic hippocampal slice cultures. Hippocampal slice cultures were biolistically transfected with the red soluble protein Tomato on DIV3 and stimulated with dihexa or HGF on DIV5. (B) Representative images of CA1 neurons from slices that were either treated with vehicle (control), 10^{-12} M dihexa, or 10 ng/ml HGF for 2 days. (C) Bar graph showing quantitated spine density per 50 μm of dendrite length for each treatment group. Dihexa and HGF significantly increased the number of spines on CA1 hippocampal neurons compared to control-treated (mean ± S.E.M.; $N = 50$; ***$P < 0.001$). (D and E) Effects of combined subthreshold doses of Nle^1-AngIV, dihexa, and HGF on spinogenesis. (D) Subthreshold levels of HGF (2.5 ng/ml) and Nle^1-AngIV (10^{-13} M) did not affect basal spine numbers. However the combination of subthreshold Nle^1-AngIV (10^{-13} M) and HGF (2.5 ng/ml) produced a significant induction of spinogenesis (***$P < 0.001$) that was equivalent to that seen with suprathreshold HGF (10 ng/ml) or Nle^1-AngIV (10^{-12} M). (E) Subthreshold levels of HGF (2.5 ng/ml) and dihexa (10^{-13} M) did not affect basal spine numbers. However the combination of subthreshold dihexa (10^{-13} M) and HGF (2.5 ng/ml) produced a significant induction of spinogenesis (***$P < 0.001$) that was equivalent to that seen with suprathreshold HGF (10 ng/ml) or dihexa (10^{-12} M). The ability of combined agonists at subthreshold doses to generate maximal responses suggests a commonality of receptor pathways. Mean ± S.E.M.; $n = 50$.

Hinge and vehicle-treated neurons (mean frequency for HGF = 9.08 ± 0.28, $n = 46$ and for dihexa = 7.93 ± 0.38, $n = 31$). These effects are significantly attenuated by stimulation in the presence of Hinge (mean frequencies for HGF + Hinge = 5.16 ± 0.27, $n = 38$, and dihexa + Hinge = 5.55 ± 0.35, $n = 29$). Together these results indicate that newly generated spines form functional synapses, and that Hinge has no effect on mEPSC frequency alone but blocks the effects of dihexa and HGF, indicating their dependence on a functional HGF/c-Met system.

To further confirm that the synaptogenic effects of dihexa and Nle^1-AngIV are HGF/c-Met system–dependent, an shRNA specific for c-Met was employed to reduce receptor expression. Dissociated hippocampal neurons were transfected with mRFP-β-actin and shMet RNA and receptor knockdown was allowed to proceed for 48 hours prior to stimulating with HGF (10 ng/ml), dihexa, or Nle^1-AngIV (both at 10^{-12} M). Neurons transfected with mRFP-β-actin alone, serving as the control, were treated with HGF, dihexa, or Nle^1-AngIV. A significant increase in the number of spines compared to control-treated neurons was observed (mean spine numbers per 50-μm dendrite length = 13.2 versus HGF = 20.6; dihexa = 21.8 and Nle^1-AngIV = 20.0; $P < 0.05$ by one-way ANOVA followed by Tukey post hoc test). The spine numbers in neurons transfected with mRFP-β-actin and the shMet, which were stimulated with 10 ng/ml HGF, 10^{-12} M dihexa, or Nle^1-AngIV, did not differ from controls (mean spine numbers per 50-μm dendrite length = 13.5 versus HGF = 12.4; dihexa = 12.0 and Nle^1-AngIV = 12.1; $P > 0.05$ by one-way ANOVA followed by Tukey post hoc test) as shown in Fig. 6H. Application of a scrambled RNA sequence, which was employed as the negative control, had no effect on basal or stimulated spinogenesis (Fig. 6H).

Because of the purposely low transfection rate required to visualize individual dendrites, direct assessment of c-Met levels in the mRFP-β-actin–labeled neurons was not feasible. Nevertheless, in an attempt to gauge the general effectiveness of shRNA,

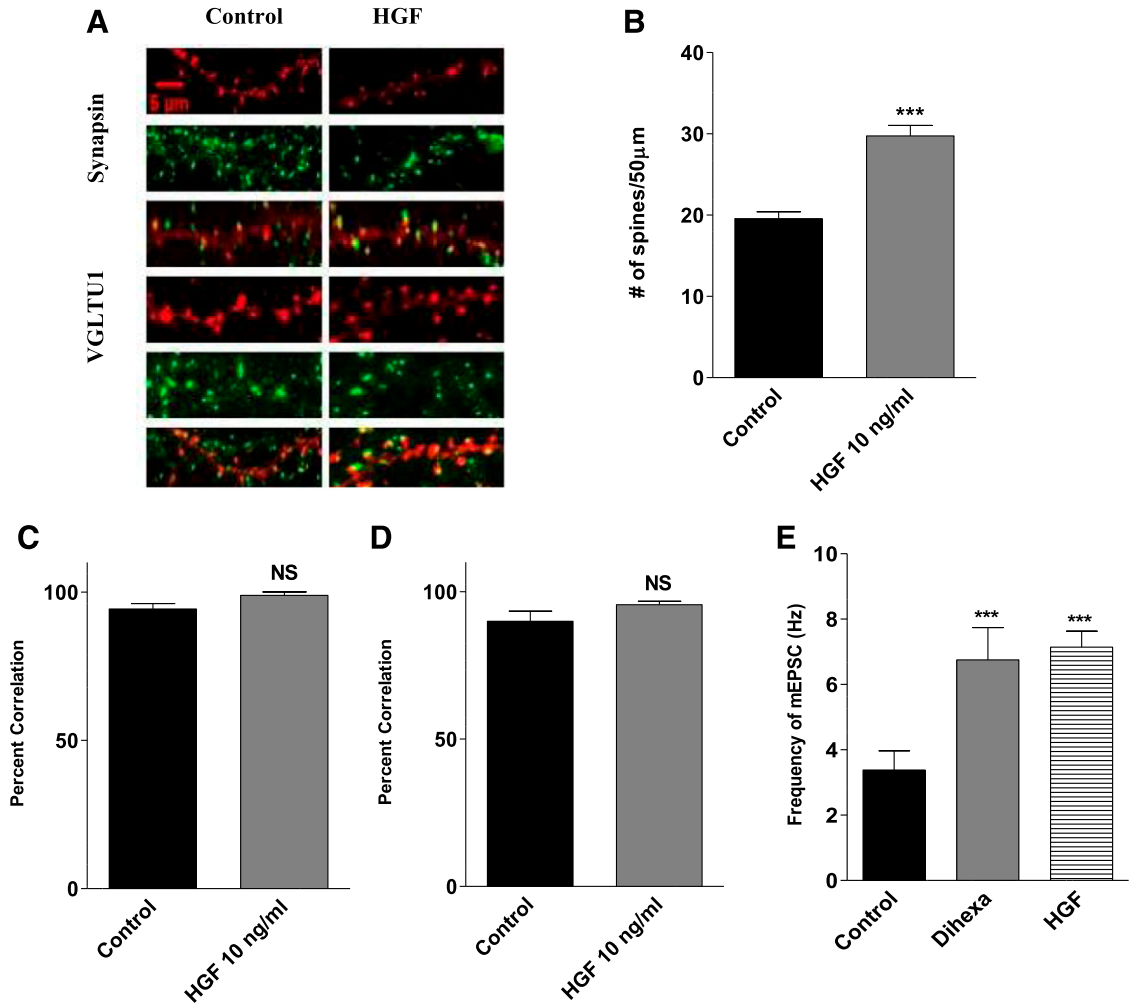

Fig. 5. Effect of HGF treatment on synaptogenesis in dissociated hippocampal neurons. HGF treatment supports the formation of functional synapses as indicated by a high correlation between postsynaptic spines (red) and markers of presynaptic active zones (green). (A) Representative images of hippocampal neurons transfected with mRFP-β-actin on DIV6 and treated with 10 ng/ml of HGF or vehicle for 5 days. The neurons were stained for the general presynaptic marker synapsin and the glutamatergic presynaptic marker VGLUT1. (B) Bar graph demonstrating an active phenotype as indicated by a significant increase in the number of spines per 50 μm of dendrite length following stimulation with HGF (10 ng/ml). Mean number of spines, HGF = 33 versus control = 23; mean ± S.E.M.; $N = 25$; ***$P < 0.001$. (C) Percent correlation of actin-enriched postsynaptic spines (red) juxtaposed to the universal presynaptic marker synapsin (green). NS = $P > 0.05$. The high percent correlation suggests functional synapses are formed. (D) Percent correlation of actin-enriched spines (red) juxtaposed to the glutamatergic presynaptic marker VGLUT1 (green). NS = $P > 0.05$. A greater than 95% correlation suggests many of these inputs are glutamatergic. (E) Effect of dihexa and HGF treatment on the frequency of mEPSCs in dissociated hippocampal neurons. Dissociated hippocampal neurons transfected with mRFP-β-actin were stimulated with 10^{-12} M dihexa or 10 ng/ml for 5 days prior to recording mEPSCs. Neurons were treated with tetrodotoxin, picrotoxin, and strychnine to block sodium channels, $GABA_A$, and glycine receptors. Treatment with both agonists significantly enhanced AMPA-receptor mediated currents compared to vehicle treated neurons Mean ± S.E.M.; $n = 9$ respectively; ***$P < 0.012$ HGF versus control; $P < 0.04$ Hex versus control). NS, not significant.

human embryonic kidney cells were transfected with 6-Myc–tagged c-Met (0.1 μg) alone, with the shMet, or with a scrambled control RNA (Fig. 6, F and G).

Together these results demonstrate that the prospinogenic/synaptogenic effects of AngIV analogs are mediated by activation of the HGF/c-Met system.

HGF Antagonist Hinge Blocks the Ability of Dihexa to Restore Cognitive Function. Previous studies from our laboratory have demonstrated that oral delivery of dihexa can normalize or improve spatial learning in scopolamine-deficit and aged-rat dementia models (McCoy et al., 2013). These results combined with the above data indicating that dihexa-mediated synaptogenesis is HGF/c-Met–dependent predicts that intracerebroventricularly delivered Hinge, an HGF antagonist, should be able to block the capacity of orally delivered dihexa to reverse scopolamine-dependent spatial learning deficits in rats. To evaluate the validity of this hypothesis, spatial learning was monitored using the Morris water maze task, a hippocampal-dependent spatial learning task requiring rats to locate a pedestal hidden beneath the surface of the water by orienting to extra-maze cues. The groups tested included a control in which aCSF was delivered intracerebroventricularly followed by oral saline; intracerebroventricular scopolamine (70 nmoles) followed by oral saline, which was expected to instigate a learning deficit; intracerebroventricular scopolamine followed by oral dihexa (2 mg/kg), which was anticipated to reverse the expected scopolamine-dependent cognitive deficit; intracerebroventricular aCSF followed by oral dihexa (2 mg/kg); intracerebroventricular Hinge (300 pmoles) followed by oral saline; and intracerebroventricular scopolamine + Hinge followed by dihexa, which was expected to blunt dihexa's ability to restore cognitive function. Figure 7 presents

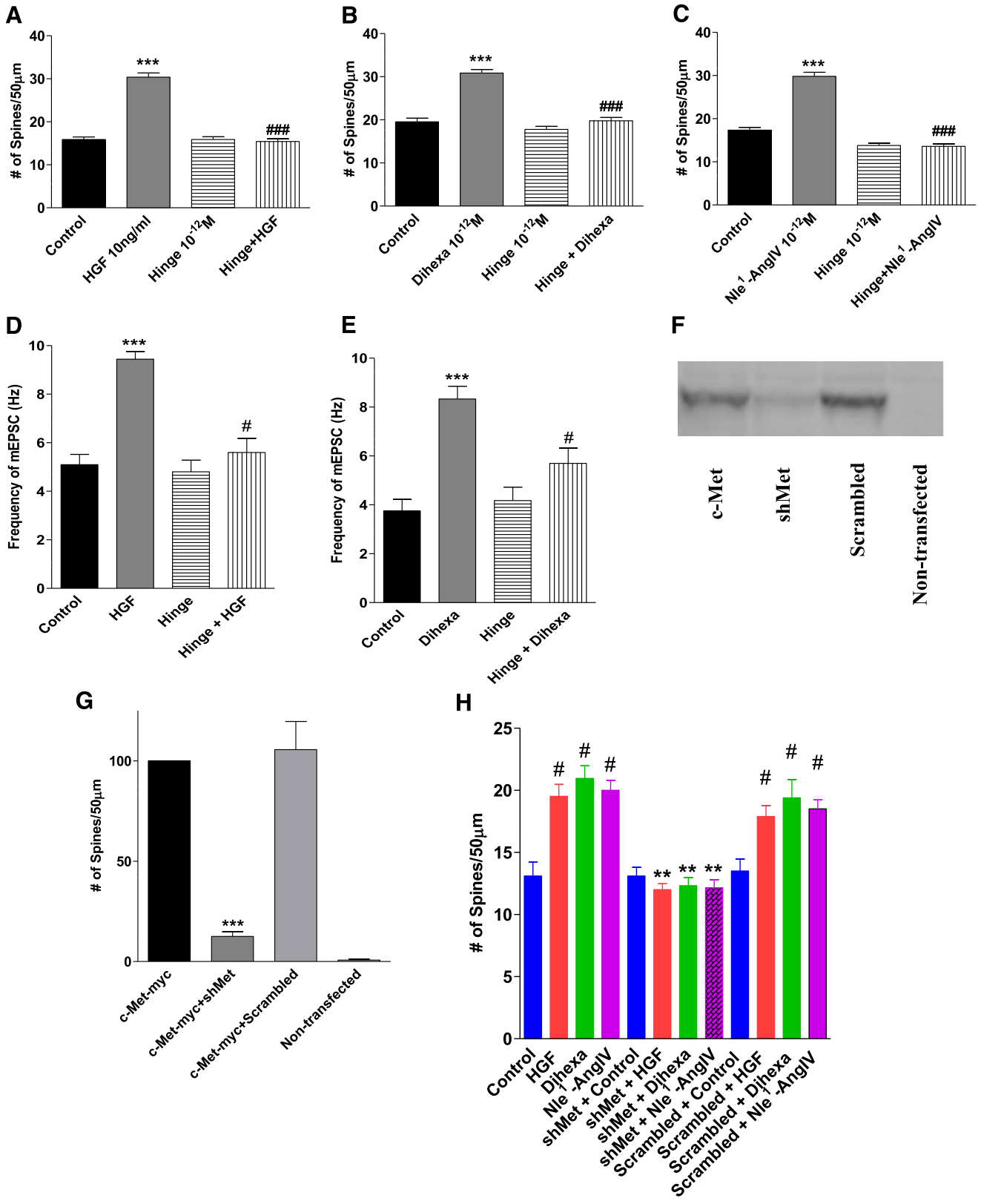

Fig. 6. Effects of the HGF antagonist Hinge and a Met shRNA on spinogenesis. Dissociated hippocampal neurons from 1- or 2-day-old rats were transfected with mRFP-β-actin and stimulated with HGF, dihexa, or Nle^1-AngIV with or without the HGF antagonist Hinge for 5 days (Kawas et al., 2011). Mean ± S.E.M.; $N = 50$). (A) As has been seen previously, HGF induced spine formation ($^{***}P < 0.001$), whereas application with Hinge had no impact on spine formation. Coapplication of Hinge with HGF, however, completely suppressed spine induction ($^{###}P < 0.001$). (B) Dihexa similarly induced spine formation ($^{***}P < 0.001$) and coapplication with Hinge reversed the effect ($^{###}P < 0.001$). (C) Likewise, Nle^1-AngIV induced spine formation ($^{***}P < 0.001$) and coapplication with Hinge reversed the effect ($^{###}P < 0.001$). In order to confirm that blockade of HGF's effect on spinogenesis by Hinge translated to a reduction in the frequency of mEPSCs, voltage-clamp recordings were made from dissociated hippocampal neurons following 5 days of treatment with drug. (D) As had been observed previously, HGF treatment increased the frequency of mEPSCs ($^{***}P < 0.001$),

the mean latencies to find the hidden pedestal in days 1–8 of training in the water maze. None of the groups differed significantly in latency to find the pedestal on day 1 of training, with mean latencies for the vehicle control (aCSF → saline) group = 71.0 seconds; the scopolamine → saline group = 109.9 seconds; the aCSF→ dihexa group = 117.5 seconds; the Hinge → saline group = 90.4 seconds; the scopolamine → dihexa group = 115.2 seconds; and, the scopolamine + Hinge → dihexa treated group = 107.9 seconds ($P > 0.05$). By the fourth day of training the scopolamine → saline group (mean latency to find the pedestal = 88.7 seconds) and the scopolamine + Hinge → dihexa group (mean latency = 78.6 seconds) showed little sign of improvement compared to the aCSF control group (mean latency = 30.4 seconds), the Hinge → saline group (mean latency = 37.2 seconds), and the scopolamine → dihexa group (mean latency = 35.5 seconds ($P < 0.05$), which were not different from one another ($P > .05$). On the final day of training, when maximal learning had occurred, the mean latencies for the scopolamine → saline group (mean latency to find the pedestal = 69.8 seconds) and the scopolamine + Hinge → dihexa group (mean latency = 71.0 seconds) were not different from one another ($P > 0.05$), indicating little improvement in learning compared to the aCSF control group (mean latency = 11.8 seconds); the Hinge → saline group (mean latency = 17.7 seconds); the aCSF → dihexa group (mean latency = 25.4 seconds); and the scopolamine → dihexa group (mean latency = 18.6 seconds). Together these data indicate that the improved cognitive function observed when dihexa was delivered orally to scopolamine-treated rats was the result of the activation of the central HGF/c-Met system.

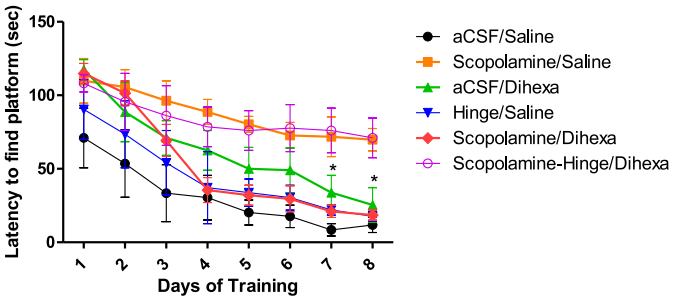

Fig. 7. Effect of HGF antagonist Hinge on dihexa's ability to restore spatial learning in the scopolamine amnesia model. Twenty minutes before beginning daily testing, 3-month-old male Sprague-Dawley rats were given scopolamine (70 nmoles) or an aCSF vehicle intracerebroventricularly followed immediately by oral delivery of dihexa (2 mg/kg) or isotonic saline. When employed, Hinge (300 pmoles) in aCSF was delivered intracerebroventricularly 5 minutes prior to testing. There were five trials per day for 8 days. The latency to find the pedestal was considered a measure of learning and memory. By day 7, oral (2 mg/kg) dihexa was able to reverse the deficit seen with scopolamine and the performance was no different than controls (*$P < 0.05$). Similarly, the aCSF/dihexa and Hinge/saline groups were not different from the control and scopolamine/dihexa groups ($P > 0.05$). By day 7, all four of these groups were different from the scopolamine-Hinge/dihexa and the scopolamine/saline groups (mean ± S.E.M.; $N = 8–10$). These data further indicate that oral dihexa enters the brain and that its effects are mediated by the central HGF/c-Met system.

Discussion

The procognitive effects of AngIV analogs have long been recognized and their potential as antidementia pharmaceuticals widely appreciated (Braszko et al., 1988; Stubley-Weatherly, 1996; Wright et al., 1999; Pederson et al., 2001; Wright and Harding, 2010). Nevertheless, two obstacles have persistently impeded the development of clinically useful analogs: 1) poor pharmacokinetic properties, and 2) the absence of an identified molecular target. The pharmacokinetic limitations of metabolic instability and an inability to pass the blood-brain barrier have recently been overcome by the design and synthesis of dihexa, a novel AngIV analog. Dihexa has documented procognitive/antidementia activity, is metabolically stable, blood-brain barrier–permeant, and orally active (McCoy et al., 2013). Here, we address the second issue that has been hindering the development of AngIV-based therapeutics, namely unknowns regarding the mechanism of action of AngIV analogs. Present results clearly demonstrate that the actions of AngIV analogs, including dihexa, are dependent on activation of the HGF/c-Met system.

Initial hints regarding the equivalency of the AngIV/AT_4 and HGF/c-Met systems can be gleaned from an examination of their physiologic signatures. Activation of the AngIV/AT_4 system is cerebroprotective (Date et al., 2004; Faure et al., 2006), augments long-term potentiation (Kramár et al., 2001; Wayner et al., 2001; Akimoto et al., 2004; Davis et al., 2006), induces dendritic and synaptic remodeling (Benoist et al., 2011; McCoy et al., 2013), stimulates hippocampal neurogenesis (L. H. Kawas and J. W. Harding, unpublished data), and has well established procognitive effects (Wright and Harding, 2010). Likewise, HGF displays profound neuroprotective activity (Shang et al., 2010; Doeppner et al., 2011) and has a proven ability both to potently stimulate neurogenesis (Nicoleau et al., 2009; Shang et al., 2010; Wang et al., 2011) and facilitate long-term potentiation (Akimoto et al., 2004). HGF is a potent neurotrophic factor in many brain regions (Ebens et al., 1996; Kato et al., 2003), affecting a variety of neuronal cell types. Activation of the HGF/c-Met system has been shown to possess neuroprotective/neurorestorative activity related to amyotrophic lateral sclerosis (Kadoyama et al., 2007), Parkinson's disease (Koike et al., 2006; Lan et al., 2008), spinal cord trauma (Kitamura et al., 2011), and multiple sclerosis (Bai et al., 2012). Moreover, activation of the HGF/c-Met system improves cognition (Akimoto et al., 2004)—an

whereas Hinge had no effect on basal frequencies. However, coapplication of Hinge with HGF suppressed the observed increase in frequencies ($^{\#}P < 0.028$) (Mean ± S.E.M.; $N = 38–46$). (E) Dihexa treatment was again found to increase the frequency of mEPSCs (***$P < 0.001$) Similarly to what was observed with the HGF treatment, coapplication of Hinge blocked the dihexa-dependent increase in frequency ($^{\#}P < 0.01$) (mean ± S.E.M.; $N = 23–44$). An shRNA targeting c-Met was designed using the RNAi central design program and inserted into the pSUPER vector under control of the H1 promoter. In order to validate the effectiveness of the shMet, HEK-293T cells were cotransfected with the shMet vector and c-Met-6-Myc–tagged pCAGGS-6-Myc destination vector. (F) As can be seen in the representative gel, the c-Met-6-Myc construct was effectively expressed compared to nontransfected controls (G; ***$P <$ 0.001; mean ± S.E.M.; $N = 4$). c-Met-6-Myc expression was significantly suppressed by cotransfection of the shMet vector (***$P < 0.001$) but not by a cotransfected scrambled oligo-containing vector ($P > 0.05$). (H) After validating the effectiveness of the shMet construct, dissociated hippocampal neurons from 1- or 2-day-old rats were transfected with mRFP-β-actin and treated with HGF, dihexa, or Nle^1-AngIV for 5 days. Some groups were cotransfected with either shMet or a scrambled control vector. HGF, dihexa, and Nle^1-AngIV all induced spine formation ($P < 0.001$), whereas shMet completely blocked spine induction by all three agonists (**$P < 0.01$); the scrambled construct had no effect ($^{\#}P > 0.05$) (mean ± S.E.M.; $N = 50$).

outcome that may reflect its ability to induce dendritic remodeling (Tyndall et al, 2007) and spur neural stem cell proliferation and differentiation (Nicoleau et al., 2009).

In addition to functional similarities, there is sequence homology between AngIV, its analogs, and a small, six-amino-acid domain of HGF termed the "hinge" region, which participates in the process of HGF dimerization (Kawas et al., 2012). Dimerization is required for HGF activation and ultimately the activation of its receptor, c-Met (Gherardi et al., 2006; Youles et al., 2008). Published studies with the AT_4 receptor antagonist norleual illustrate its ability to bind to HGF with high affinity, compete for the binding of a "hinge" peptide to HGF, and allosterically inhibit the ability of HGF to activate c-Met and induce cellular responses (Yamamoto et al., 2010; Kawas et al., 2011, 2012).

We hypothesize that AngIV analogs, such as Nle^1-AngIV and dihexa, bind to and allosterically activate HGF better than HGF itself, forming an active heterodimer of HGF-dihexa. Further, we believe that HGF dimerization is a process designed to yield an active HGF conformation and not as typically suggested to mediate receptor dimerization. This supposition is based on our recent demonstration that, at least in rat hippocampal neurons, c-Met is premultimerized at postsynaptic densities as dimers, tetramers, hexamers, and octomers in the absence of HGF (Kawas et al., 2013). Since the receptors are already assembled, an HGF-mediated receptor dimerization process would be unnecessary and suggests that HGF dimerization may have another physiological role, namely to induce the active conformation of HGF. In concert with this hypothesis, regarding dihexa's positive allosterism, we found that dihexa bound to HGF with high affinity (Fig. 1A), disrupted HGF-HGF dimerization (Fig. 1B), but resulted in a leftward shift of the HGF dose-response curve and augmentation of HGF's biological activity, even at subthreshold concentrations of HGF (Figs. 2 and 3).

If as hypothesized, the action of procognitive AngIV analogs is mediated through activation of the HGF/c-Met system, and since multiple AngIV analogs have previously been shown to stimulate dendritic spine growth in dissociated hippocampal neurons (Benoist et al., 2011; McCoy et al., 2013), we anticipated that HGF should exhibit similar activity. As predicted, HGF promoted a dose-dependent increase in spinogenesis in dissociated hippocampal neurons that yielded functional synaptic connections (Fig. 4A). The most effective concentration of HGF (10 ng/ml) was subsequently found to stimulate spinogenesis in hippocampal neurons in organotypic hippocampal slice cultures, which represent a more intact preparation (Fig. 4, B and C).

Most importantly to our hypothesis, the HGF antagonist Hinge (Kawas et al., 2011) inhibited the spinogenic activity of HGF, Nle^1-AngIV, and dihexa (Fig. 6, A–C). Hinge, like norleual, was established as an HGF antagonist based on its ability to bind HGF, inhibit HGF dimerization, block HGF-dependent c-Met phosphorylation, and prevent HGF-dependent scattering in the MDCK epithelial cell line (Kawas et al., 2012). In concert with these data, transfection of rat hippocampal neurons with a c-Met shRNA similarly attenuated HGF-, Nle^1-AngIV–, and dihexa-dependent spinogenesis (Fig. 6, F–H), thus substantiating the functional linkage between procognitive AngIV analogs and the HGF/c-Met system. The concomitant ability of Hinge to block HGF- and dihexa-stimulated increase in mEPSC frequency in hippocampal neurons (Fig. 6, D and E) further indicates that Nle^1-AngIV– and dihexa-dependent synaptogenesis is HGF dependent.

Despite Hinge's ability to block the capacity of HGF, Nle^1-AngIV, and dihexa to induce spinogenesis and synaptogenesis, Hinge had no effect on basal spinogenesis or synaptogenesis in cultured hippocampal neurons, suggesting that endogenous levels of HGF in the cultures were below the threshold concentration required for both processes (Fig. 6, D and H). Likewise, neither the HGF antagonist nor c-Met shRNA impacted basal levels of spinogenesis in the cultures. The observed capability of Nle^1-AngIV and dihexa to induce spinogenesis and synaptogenesis in these same cultures offers additional support for the notion that both act by shifting HGF's dose-response curve to the left and render biologically subthreshold levels of HGF physiologically meaningful.

Dihexa has recently been shown to augment the cognitive abilities of aged and scopolamine-treated rats as assessed using the Morris water maze task (McCoy et al., 2013). In order to expand our appraisal of the mechanism of action of procognitive AngIV analogs to an in vivo setting, we evaluated the ability of Hinge to alter the procognitive/antidementia action of dihexa. Using an experimental paradigm identical to that employed in the McCoy et al. (2013) study, cognitive deficits were induced by intracerebroventricular application of the muscarinic receptor antagonist scopolamine, which renders rats acutely amnesic and therefore unable to learn the water maze task. As previously reported (McCoy et al., 2013), orally delivered dihexa reversed the cognitive deficits observed following scopolamine pretreatment. Most importantly, intracerebroventricular coapplication of Hinge with scopolamine blocked the capacity of dihexa to rescue water maze performance. Application of Hinge alone had no impact on basal performance, suggesting that the HGF/c-Met system is not engaged during normal learning. This is consistent with previous Morris water maze results indicating that treatment with AngIV, or AngIV analogs, failed to facilitate learning and memory in normal functioning animals (Wright et al., 1999). Alternatively, the consistent ability of an augmented HGF/c-Met system to support synaptic plasticity and to reverse nervous system deficits as documented here and by others suggests that the HGF/c-Met system is designed to respond to injury when markedly enhanced synaptic plasticity is beneficial, as seen in stroke and neurodegenerative diseases. This notion is further supported by elevations in central nervous system HGF levels observed in several degenerative diseases (Kato et al., 2003; Shimamura et al., 2007; Salehi and Rajaei, 2010; Muller et al., 2012), perhaps representing the brain's or spinal cord's attempt to activate regenerative processes.

In summary, results presented here and elsewhere (Yamamoto et al., 2010; Kawas et al., 2011, 2012) support the hypothesis that the biologic actions of AngIV analogs, including those that are procognitive, are dependent on interaction with HGF and subsequent modulation of c-Met activity. Furthermore these data are consistent with an allosteric model in which AngIV analogs bind to HGF inducing a conformational change. The presence of both high-affinity HGF antagonists and activators that inhibit dimerization suggests that singlet HGF is capable of activating c-Met and that the function of dimerization is to support the active conformation of HGF. Ultimately, biophysical and structural studies will be needed to unequivocally confirm this allosteric model.

Authorship Contributions

Participated in research design: Benoist, Kawas, Harding, Wayman, Wright, Appleyard.

Conducted experiments: Benoist, Kawas, Zhu, Wright, Stillmaker, Tyson.

Contributed new reagents or analytic tools: Harding.

Performed data analysis: Benoist, Kawas, Zhu, Harding, Wright, Tyson.

Wrote or contributed to the writing of the manuscript: Harding, Benoist, Kawas, Zhu, Wright, Wayman, Appleyard.

References

Akimoto M, Baba A, Ikeda-Matsuo Y, Yamada MK, Itamura R, Nishiyama N, Ikegaya Y, and Matsuki N (2004) Hepatocyte growth factor as an enhancer of nmda currents and synaptic plasticity in the hippocampus. *Neuroscience* **128**:155–162.

Albiston AL, McDowall SG, Matsacos D, Sim P, Clune E, Mustafa T, Lee J, Mendelsohn FA, Simpson RJ, and Connolly LM, et al. (2001) Evidence that the angiotensin IV (AT(4)) receptor is the enzyme insulin-regulated aminopeptidase. *J Biol Chem* **276**: 48623–48626.

Albiston AL, Fernando RN, Yeatman HR, Burns P, Ng L, Daswani D, Diwakarla S, Pham V, and Chai SY (2010) Gene knockout of insulin-regulated aminopeptidase: loss of the specific binding site for angiotensin IV and age-related deficit in spatial memory. *Neurobiol Learn Mem* **93**:19–30.

Bai L, Lennon DP, Caplan AI, DeChant A, Hecker J, Kranso J, Zaremba A, and Miller RH (2012) Hepatocyte growth factor mediates mesenchymal stem cell–induced recovery in multiple sclerosis models. *Nat Neurosci* **15**:862–870.

Balschun D, Moechars D, Callaerts-Vegh Z, Vermaercke B, Van Acker N, Andries L, and D'Hooge R (2010) Vesicular glutamate transporter VGLUT1 has a role in hippocampal long-term potentiation and spatial reversal learning. *Cereb Cortex* **20**: 684–693.

Benoist CC, Wright JW, Zhu M, Appleyard SM, Wayman GA, and Harding JW (2011) Facilitation of hippocampal synaptogenesis and spatial memory by C-terminal truncated Nle1-angiotensin IV analogs. *J Pharmacol Exp Ther* **339**:35–44.

Braszko JJ, Kupryszewski G, Witczuk B, and Wiśniewski K (1988) Angiotensin II-(3-8)-hexapeptide affects motor activity, performance of passive avoidance and a conditioned avoidance response in rats. *Neuroscience* **27**:777–783.

Chen JK, Zimpelmann J, Harris RC, and Burns KD (2001) Angiotensin IV induces tyrosine phosphorylation of focal adhesion kinase and paxillin in proximal tubule cells. *Am J Physiol Renal Physiol* **280**:F980–F988.

Date I, Takagi N, Takagi K, Kago T, Matsumoto K, Nakamura T, and Takeo S (2004) Hepatocyte growth factor improved learning and memory dysfunction of microsphere-embolized rats. *J Neurosci Res* **78**:442–453.

Davis CJ, Kramár EA, De A, Meighan PC, Simasko SM, Wright JW, and Harding JW (2006) AT_4 receptor activation increases intracellular calcium influx and induces a non-N-methyl-D-aspartate dependent form of long-term potentiation. *Neuroscience* **137**:1369–1379.

Doeppner TR, Kaltwasser B, ElAli A, Zechariah A, Hermann DM, and Bähr M (2011) Acute hepatocyte growth factor treatment induces long-term neuroprotection and stroke recovery via mechanisms involving neural precursor cell proliferation and differentiation. *J Cereb Blood Flow Metab* **31**:1251–1262.

Ebens A, Brose K, Leonardo ED, Hanson MG, Jr, Bladt F, Birchmeier C, Barres BA, and Tessier-Lavigne M (1996) Hepatocyte growth factor/scatter factor is an axonal chemoattractant and a neurotrophic factor for spinal motor neurons. *Neuron* **17**: 1157–1172.

Faure S, Chapot R, Tallet D, Javellaud J, Achard JM, and Oudart N (2006) Cerebroprotective effect of angiotensin IV in experimental ischemic stroke in the rat mediated by $AT_{(4)}$ receptors. *J Physiol Pharmacol* **57**:329–342.

Ferreira A and Rapoport M (2002) The synapsins: beyond the regulation of neurotransmitter release. *Cell Mol Life Sci* **59**:589–595.

Gherardi E, Sandin S, Petoukhov MV, Finch J, Youles ME, Ofverstedt LG, Miguel RN, Blundell TL, Vande Woude GF, and Skoglund U, et al. (2006) Structural basis of hepatocyte growth factor/scatter factor and MET signalling. *Proc Natl Acad Sci USA* **103**:4046–4051.

Hamilton TA, Handa RK, Harding JW, and Wright JW (2001) A role for the angiotensin IV/AT_4 system in mediating natriuresis in the rat. *Peptides* **22**:935–944.

Handa RK (2001) Characterization and signaling of the AT(4) receptor in human proximal tubule epithelial (HK-2) cells. *J Am Soc Nephrol* **12**:440–449.

Kadoyama K, Funakoshi H, Ohya W, and Nakamura T (2007) Hepatocyte growth factor (HGF) attenuates gliosis and motoneuronal degeneration in the brainstem motor nuclei of a transgenic mouse model of ALS. *Neurosci Res* **59**:446–456.

Kato S, Funakoshi H, Nakamura T, Kato M, Nakano I, Hirano A, and Ohama E (2003) Expression of hepatocyte growth factor and c-Met in the anterior horn cells of the spinal cord in the patients with amyotrophic lateral sclerosis (ALS): immunohistochemical studies on sporadic ALS and familial ALS with superoxide dismutase 1 gene mutation. *Acta Neuropathol* **106**:112–120.

Kawas LH, Yamamoto BJ, Wright JW, and Harding JW (2011) Mimics of the dimerization domain of hepatocyte growth factor exhibit anti-Met and anticancer activity. *J Pharmacol Exp Ther* **339**:509–518.

Kawas LH, McCoy AT, Yamamoto BJ, Wright JW, and Harding JW (2012) Development of angiotensin IV analogs as hepatocyte growth factor/Met modifiers. *J Pharmacol Exp Ther* **340**:539–548.

Kawas LH, Benoist CC, Harding JW, Wayman GA, and Abu-Lail NI (2013) Nanoscale mapping of the Met receptor on hippocampal neurons by AFM and confocal microscopy. *Nanomedicine (Lond Print)* **9**:428–438.

Kitamura K, Fujiyoshi K, Yamane J, Toyota F, Hikishima K, Nomura T, Funakoshi H, Nakamura T, Aoki M, and Toyama Y, et al. (2011) Human hepatocyte growth factor promotes functional recovery in primates after spinal cord injury. *PLoS ONE* **6**:e27706.

Koike H, Ishida A, Shimamura M, Mizuno S, Nakamura T, Ogihara T, Kaneda Y, and Morishita R (2006) Prevention of onset of Parkinson's disease by in vivo gene transfer of human hepatocyte growth factor in rodent model: a model of gene therapy for Parkinson's disease. *Gene Ther* **13**:1639–1644.

Kramár EA, Harding JW, and Wright JW (1997) Angiotensin II- and IV-induced changes in cerebral blood flow. Roles of AT_1, AT_2, and AT_4 receptor subtypes. *Regul Pept* **68**:131–138.

Kramár EA, Armstrong DL, Ikeda S, Wayner MJ, Harding JW, and Wright JW (2001) The effects of angiotensin IV analogs on long-term potentiation within the CA1 region of the hippocampus in vitro. *Brain Res* **897**:114–121.

Lan F, Xu J, Zhang X, Wong VW, Li X, Lu A, Lu W, Shen L, and Li L (2008) Hepatocyte growth factor promotes proliferation and migration in immortalized progenitor cells. *Neuroreport* **19**:765–769.

Li YD, Block ER, and Patel JM (2002) Activation of multiple signaling modules is critical in angiotensin IV-induced lung endothelial cell proliferation. *Am J Physiol Lung Cell Mol Physiol* **283**:L707–L716.

McCoy AT, Benoist CC, Wright JW, Kawas LH, Bule-Ghogare JM, Zhu M, Appleyard SM, Wayman GA, and Harding JW (2013) Evaluation of metabolically stabilized angiotensin IV analogs as procognitive/antidementia agents. *J Pharmacol Exp Ther* **344**:141–154.

Müller AM, Jun E, Conlon H, and Sadiq SA (2012) Cerebrospinal hepatocyte growth factor levels correlate negatively with disease activity in multiple sclerosis. *J Neuroimmunol* **251**:80–86.

Nicoleau C, Benzakour O, Agasse F, Thiriet N, Petit J, Prestoz L, Roger M, Jaber M, and Coronas V (2009) Endogenous hepatocyte growth factor is a niche signal for subventricular zone neural stem cell amplification and self-renewal. *Stem Cells* **27**: 408–419.

Peters S and Adjei AA (2012) MET: a promising anticancer therapeutic target. *Nat Rev Clin Oncol* **9**:314–326.

Pederson ES, Krishnan R, Harding JW, and Wright JW (2001) A role for the angiotensin AT_4 receptor subtype in overcoming scopolamine-induced spatial memory deficits. *Regul Pept* **102**:147–156.

Salehi Z and Rajaei F (2010) Expression of hepatocyte growth factor in the serum and cerebrospinal fluid of patients with Parkinson's disease. *J Clin Neurosci* **17**: 1553–1556.

Shang J, Deguchi K, Yamashita T, Ohta Y, Zhang H, Morimoto N, Liu N, Zhang X, Tian F, and Matsuura T, et al. (2010) Antiapoptotic and antiautophagic effects of glial cell line-derived neurotrophic factor and hepatocyte growth factor after transient middle cerebral artery occlusion in rats. *J Neurosci Res* **88**:2197–2206.

Shimamura M, Sato N, Sata M, Wakayama K, Ogihara T, and Morishita R (2007) Expression of hepatocyte growth factor and c-Met after spinal cord injury in rats. *Brain Res* **1151**:188–194.

Stella MC and Comoglio PM (1999) HGF: a multifunctional growth factor controlling cell scattering. *Int J Biochem Cell Biol* **31**:1357–1362.

Stubley-Weatherly L, Harding JW, and Wright JW (1996) Effects of discrete kainic acid-induced hippocampal lesions on spatial and contextual learning and memory in rats. *Brain Res* **716**:29–38.

Tyndall SJ, Patel SJ, and Walikonis RS (2007) Hepatocyte growth factor-induced enhancement of dendritic branching is blocked by inhibitors of N-methyl-D-aspartate receptors and calcium/calmodulin-dependent kinases. *J Neurosci Res* **85**: 2343–2351.

Wang TW, Zhang H, Gyetko MR, and Parent JM (2011) Hepatocyte growth factor acts as a mitogen and chemoattractant for postnatal subventricular zone-olfactory bulb neurogenesis. *Mol Cell Neurosci* **48**:38–50.

Wayman GA, Impey S, Marks D, Saneyoshi T, Grant WF, Derkach V, and Soderling TR (2006) Activity-dependent dendritic arborization mediated by CaM-kinase I activation and enhanced CREB-dependent transcription of Wnt-2. *Neuron* **50**: 897–909.

Wayman GA, Davare M, Ando H, Fortin D, Varlamova O, Cheng HY, Marks D, Obrietan K, Soderling TR, and Goodman RH, et al. (2008) An activity-regulated microRNA controls dendritic plasticity by down-regulating p250GAP. *Proc Natl Acad Sci USA* **105**:9093–9098.

Wayner MJ, Armstrong DL, Phelix CF, Wright JW, and Harding JW (2001) Angiotensin IV enhances LTP in rat dentate gyrus in vivo. *Peptides* **22**:1403–1414.

Wright JW and Harding JW (2010) The brain RAS and Alzheimer's disease. *Exp Neurol* **223**:326–333.

Wright JW and Harding JW (2013) The brain renin-angiotensin system: a diversity of functions and implications for CNS diseases. *Pflugers Arch* **465**:133–151.

Wright JW, Stubley L, Pederson ES, Kramár EA, Hanesworth JM, and Harding JW (1999) Contributions of the brain angiotensin IV-AT_4 receptor subtype system to spatial learning. *J Neurosci* **19**:3952–3961.

Yamamoto BJ, Elias PD, Masino JA, Hudson BD, McCoy AT, Anderson ZJ, Varnum MD, Sardinia MF, Wright JW, and Harding JW (2010) The angiotensin IV analog Nle-Tyr-Leu-psi-(CH2-NH2)3-4-His-Pro-Phe (norleual) can act as a hepatocyte growth factor/c-Met inhibitor. *J Pharmacol Exp Ther* **333**:161–173.

Youles M, Holmes O, Petoukhov MV, Nessen MA, Stivala S, Svergun DI, and Gherardi E (2008) Engineering the NK1 fragment of hepatocyte growth factor/scatter factor as a MET receptor antagonist. *J Mol Biol* **377**:616–622.

Zhang YW and Vande Woude GF (2003) HGF/SF-met signaling in the control of branching morphogenesis and invasion. *J Cell Biochem* **88**:408–417.

Address correspondence to: Dr. Joseph W. Harding or Dr. Gary A. Wayman, Department of Integrative Physiology and Neuroscience, Washington State University, Pullman, WA 99164-6520. E-mail: hardingj@vetmed.wsu.edu or waymang@vetmed.wsu.edu